

An Enhanced Interleaved Chirp Spreading LoRa Modulation Scheme for High Data Transmission

Yu Shi*, Weikai Xu*, Member, IEEE, Lin Wang*, Senior Member, IEEE

*Dept. of Information and Communication Engineering, Xiamen University, Xiamen, 361005, Fujian, China.

Email: xweikai@xmu.edu.cn

Abstract—LoRa is a technology based on the physical layer with chirp spread spectrum (CSS) as the backbone. It relies on different spreading factors (SF) to spread signals over the entire bandwidth. At the same time, the SF restricts the number of bits contained in each LoRa symbol, making LoRa has limited transmission capacity. This paper proposes an enhanced interleaved chirp spread LoRa (EICS-LoRa) scheme, which aims to increase the transmission rate of the LoRa network. In EICS-LoRa, an interleaver selected from 2^r candidate interleavers is used to interleave LoRa symbol. Since r bits are used to determine the choice of interleaver, r more bits are carried on each LoRa symbol. The simulation results show that the performance gap between Nominal LoRa and EICS-LoRa increases when the parameter r increases. However the rate gain improves significantly with the increase of r . In addition, the simulation results with the same spreading factor (co-SF) interference show that EICS-LoRa has better resistance to co-SF interference than LoRa due to inherent interleaving.

Index Terms—LoRa modulation, interleaving, bit-error-ratio, co-SF interference

I. INTRODUCTION

Internet of Things (IoT) is developing rapidly and has been applied to an increasing number of fields, such as smart city, traffic control, intelligent agriculture, etc. [1]. In order to solve the trade-off problem between transmission distance and energy consumption, low power wide area networks (LP-WAN) have emerged and gained wide attention from researchers [2], [3]. Long communication distance and low power consumption are the biggest features of LP-WAN technologies. The main LP-WAN technologies currently on the market include NB-IoT, LoRa, SigFox, etc. [4]. LoRa (Long Range) has made itself one of the most potential technology among LP-WAN technologies. The success of LoRa is its adaptive data rate chirp spread spectrum (CSS) modulation technology which supports energy-efficient long-range communication [5]. In the LoRa, a variable spreading factor (SF) is used to spread a narrow-band signal over a wide bandwidth to make the signal more robust to noise. It should be noted that the increase of SF will reduce the transmission rate while expanding the communication range [6].

The data rate of LoRa modulation is mainly limited by SF and the occupied bandwidth. Given the bandwidth and symbol duration, the number of orthogonal frequency shift chirps is limited. This makes the data rate of LoRa modulation relatively low [7], [8]. For this reason, more and more researches are focused on how to improve the data rate of conventional LoRa modulation. For example, in [9] and [10],

bits are embedded in the initial phase of linear up chirps to carry additional information. However, the embedded bits in the phase require channel estimation at the receiver, which will increase the complexity of the receiver [7]. In [11], linear down chirps and up chirps are used at the same time to increase the transmission data rate. But this scheme only carries one extra bit of each symbol and the transmission rate gain is very limited.

In [12], an interleaved chirp spreading LoRa (ICS-LoRa) scheme was proposed. In this scheme, the conventional LoRa chirp signal and its interleaved copy are in turn transmitted according to an extra bit. The simulation results showed that this scheme has a good performance in improving the transmission rate with sacrificing a certain sensitivity. However, ICS-LoRa only has a single interleaving mode, which results in only one extra bit being carried. When SF is large, the improvement of transmission rate is very small.

In this paper, an enhanced interleaved chirp spreading LoRa (EICS-LoRa) scheme is proposed to overcome the weakness. In the proposed EICS-LoRa scheme, interleaved LoRa chirp signals are created by new multidimensional space. The enhancement lies in the use of multiple different interleaved LoRa chirp signals which are generated by randomly commuting segments of LoRa chirp. The more interleaved chirp signals are used, the more additional bits each LoRa symbol are carried. It is shown that the maximum rate gain of 71.43% over conventional LoRa could be obtained in the cost of sacrificing about 1.72dB the sensitivity. A good trade-off could be achieved when SF is increased. Moreover, we compare the influence of the same spreading factor (co-SF) interference on EICS-LoRa and LoRa. The sensitivity loss of the EICS-LoRa scheme is less than that of LoRa at the same constraints, which means that the proposed EICS-LoRa scheme has better resistance to co-SF interference.

The rest of the paper is organized as follows. An overview of LoRa and ICS-LoRa is presented in Section II. In Section III, the system model of the proposed scheme is illustrated. Simulation results of BER performance and the ability to resist co-SF interference of the EICS-LoRa scheme are presented in Section IV. Finally, Section V concludes the paper.

II. OVERVIEW OF LORA AND ICS-LORA

A. LoRa Modulation and Demodulation

In LoRa modulation, the frequency of chirp signal changes linearly over time so as to broaden the spectrum of the signal

from 0 to the bandwidth B within a symbol duration T_s [13]. The discrete frequency function of CSS signal is given as

$$\omega_0(nT) = \sqrt{\frac{1}{2^f}} \exp[j2\pi \cdot \frac{(nT)^2}{2} \cdot \frac{B}{T_s}], \quad (1)$$

where $n = 0, 1, 2, \dots, 2^f - 1$ is the index of the sample at time $t = nT$ ($T = 1/B$ is the sample interval), and f equals SF which indicates there are 2^f samples among one symbol duration T_s ($T_s = 2^f \cdot T$). Let $T = 1$, the CSS signal $\omega_0(nT)$ could be further simplified as

$$\omega_0(n) = \sqrt{\frac{1}{2^f}} \exp[j2\pi \cdot \frac{n^2}{2^{f+1}}]. \quad (2)$$

Let $\omega_m(n)$ ($m \in M = \{0, 1, 2, \dots, 2^f - 1\}$) to represent the m th cyclic time shift of the basis signal $\omega_0(n)$ then it is expressed as

$$\omega_m(n) = \sqrt{\frac{1}{2^f}} \exp \left[j2\pi \cdot \frac{(m+n)\text{mod}(2^f)^2}{(2^{f+1})} \right], \quad (3)$$

where the symbol m is formed using a vector of f (usually ranges in $\{7, 8, 9, 10, 11, 12\}$) length bits and the relation formula is $m = \sum_{h=0}^{f-1} X_h \cdot 2^h$ [5].

Considering LoRa modulated signal that passed through AWGN channel, the received signal is expressed as

$$r(n|\Omega_l) = \sqrt{E_S} \cdot \omega_l(n) + \eta_n, \quad (4)$$

where $r(n|\Omega_l)$ is the received signal given that symbol Ω_l is transmitted, while E_S is the symbol energy and η_n is the complex Gaussian noise process [12]. The first step of demodulation is dechirping which is achieved by multiplying the received signal by the complex conjugate version of the basis signal $\omega_0(n)$,

$$\bar{r}(n|\Omega_l) = r(n|\Omega_l) \times \omega_0^*(n), \quad (5)$$

where Ω_l is the non-binary transmitted symbol and $\omega_0^*(n)$ denotes the complex conjugate of the basis signal $\omega_0(n)$ [5].

Discrete Fourier transform (DFT) is then applied to the dechirped signal $\bar{r}(n|\Omega_l)$ and in turn this operation generates 2^f outputs as

$$\mathcal{R}_{k|\Omega_l} = \mathcal{F}_k(\bar{r}(n|\Omega_l)) \cdot \sqrt{E_S} + \sum_{m=0}^{2^f-1} \eta_m \cdot \mathcal{F}_k(\bar{r}(n|\Omega_l)), \quad (6)$$

where $\mathcal{R}_{k|\Omega_l}$ ($k \in K = \{0, 1, 2, \dots, 2^f - 1\}$) means the k th DFT output of $\bar{r}(n|\Omega_l)$ and $\mathcal{F}_k(\bar{r}(n|\Omega_l))$ ($k \in K, \forall m \in M = \{0, 1, 2, \dots, 2^f - 1\}$) means the k th DFT output of the dechirped signal $\bar{r}(n|\Omega_l)$. According to [12], the magnitudes of $\mathcal{R}_{k|\Omega_l}$ could be given as

$$|\mathcal{R}_{k|\Omega_l}| = \begin{cases} |\sqrt{E_S} + \eta_l| & k = l \\ |\eta_l| & k \neq l. \end{cases} \quad (7)$$

Finally, the detected symbol \hat{l} is attained by comparing the magnitudes of $\mathcal{R}_{k|\Omega_l}$ as

$$\hat{l} = \arg_k \max(|\mathcal{R}_{0|\Omega_l}|, \dots, |\mathcal{R}_{k|\Omega_l}|, \dots, |\mathcal{R}_{2^f-1|\Omega_l}|). \quad (8)$$

The error between the non-binary transmitted symbol l with the detected symbol \hat{l} is mainly caused by the noise which defeats the magnitude of transmitted signal at the l th output.

B. ICS-LoRa Modulation and Demodulation

The transmitted rate of LoRa modulation is bound to the parameter SF. In [12], the proposed ICS-LoRa scheme is devised to carry an additional bit per symbol by introducing an interleaver. ICS-LoRa uses an interleaver to subdivide the modulated LoRa signal $\omega_l(n)$ into four parts evenly and then swaps the middle two parts. And all segments are composed of 2^{f-2} samples.

Let us use $\omega_l^{(I)}(n)$ to represent the interleaved version of LoRa signal $\omega_l(n)$ and the interleaved signal is given as

$$\omega_l^{(I)}(n) = \begin{cases} \omega_l(n) & 0 \leq n < 2^{f-2} \\ \omega_l(n+2^{f-2}) & 2^{f-2} \leq n < 2^{f-1} \\ \omega_l(n-2^{f-2}) & 2^{f-1} \leq n < 3 \times 2^{f-2} \\ \omega_l(n) & 3 \times 2^{f-2} \leq n < 2^f. \end{cases} \quad (9)$$

The interleaving process is shown in Fig. 1. It presents an example of the basis LoRa chirp signal $\omega_0(n)$ on the left and its interleaved version on the right, with $f = 7$.

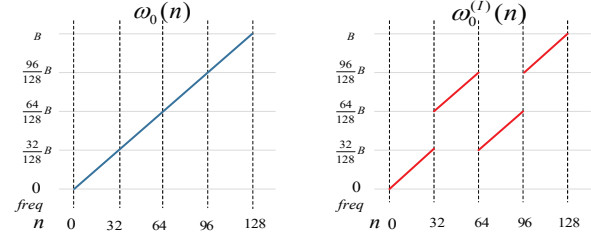


Fig. 1. The example of signals $\omega_0(n)$ and $\omega_0^{(I)}(n)$ with $f = 7$.

At the transmitter side, ICS-LoRa accepts a bits vector $X = [x_0, x_1, \dots, x_f]$ which is composed of $f + 1$ bits. The most significant f bits $[x_1, \dots, x_f]$ are carried by LoRa chirp signal. Simultaneously, the additional bit x_0 is used to decide whether use the interleaved chirp signal or not. When $x_0 = 0$, the modulated signal $\omega_l(n)$ is transmitted. When $x_0 = 1$, $\omega_l(n)$ is interleaved and the interleaved signal $\omega_l^{(I)}(n)$ is transmitted.

At the receiver, the received signal $r_{ICS}(n)$ first passes through the same interleaver as the transmitter side to produce an interleaved received signal $r_{ICS}^{(I)}(n)$. Next, dechirping needs to be applied to both the received signal $r_{ICS}(n)$ and the interleaved received signal $r_{ICS}^{(I)}(n)$. Then, the dechirped signals $\bar{r}_{ICS}(n)$ and $\bar{r}_{ICS}^{(I)}(n)$ respectively go through the DFT blocks to generate two vectors $\mathcal{R} = [\mathcal{R}_0, \mathcal{R}_1, \dots, \mathcal{R}_{2^f-1}]$ and $\mathcal{R}^{(I)} = [\mathcal{R}_0^{(I)}, \mathcal{R}_1^{(I)}, \dots, \mathcal{R}_{2^f-1}^{(I)}]$. The extra bit and transmitted symbol of ICS-LoRa are detected by

$$\hat{x}_0 = \begin{cases} 0 & \max(|\mathcal{R}|) > \max(|\mathcal{R}^{(I)}|) \\ 1 & \max(|\mathcal{R}|) < \max(|\mathcal{R}^{(I)}|) \end{cases}, \quad (10)$$

$$\hat{l} = \begin{cases} \arg \max(|\mathcal{R}|), & \max(|\mathcal{R}|) > \max(|\mathcal{R}^{(I)}|) \\ \arg \max(|\mathcal{R}^{(I)}|), & \max(|\mathcal{R}|) < \max(|\mathcal{R}^{(I)}|) \end{cases}, \quad (11)$$

where the estimated bit \hat{x}_0 is corresponding to the additional bit of the transmitted vector X . The f most significant bits are attained by using the non-binary decoder and the final estimated result of vector \hat{X} is composed of both two parts.

III. ENHANCED INTERLEAVED CHIRP SPREADING LORA SCHEME

A. Interleavers Design and Modulation of EICS-LoRa

As shown in Sub-section II-B, an interleaver is introduced in the ICS-LoRa modulation method. That is, the two middle parts of the symbols with indexes 2 and 3 are exchanged, so that each symbol could transmit one more bit [12].

Taking the LoRa symbol divided into four segments as an example, the symbol has 24 (the factorial of four) interleaving modes. So there are 24 ($4!$) possible interleavers. Considering interleavers starting with the same number (for example, starting with 1) are used in the proposed EICS-LoRa scheme, at most four candidate interleavers could be used to interleave LoRa symbols. The transmitter needs two bits to encode these interleaved LoRa chirp signals, so two extra bits are carried with each symbol. Table I shows the possible interleavers.

TABLE I
A SET OF INTERLEAVERS FOR DIVIDING A SYMBOL INTO FOUR SEGMENTS

Index	Interleaver			
0	1	3	2	4
1	1	4	3	2
2	1	2	4	3
3	1	2	3	4

Based on the above example, the design could be extended to more situations. For example, if the LoRa chirp symbol is divided into eight segments, there are 40,320 different combinations. Considering only the interleaving patterns starting with 1, there are still 5,040 candidate interleavers. In this case, at most 12 extra bits are used to encode the interleaved LoRa chirp signals. In other words, by dividing the symbol into eight segments, the transmission rate of the system could be increased by up to 12 bits per symbol.

Considering the increasing of implementation complexity and the bit error rate (BER) with the increasing of the number of interleavers, we most select 32 candidate interleavers in this paper. That means the transmission rate of the proposed scheme can promote 5 bits per symbol at most. Table II shows a set of eight interleavers for situation that a LoRa symbol is divided into eight segments.

In the proposed EICS-LoRa scheme, the first step of interleaving is to randomly generate 2^r interleavers (r is the number of additional bits per symbol), and to divide the LoRa chirp symbol into M (four or eight) segments averagely which are labelled from zero to $M-1$. When $r = 2$, $M = 4$; when $2 < r \leq 5$, $M = 8$. Then, the LoRa chirp symbol are rearranged in the order of the selected interleaver. Figure 2 shows an example that the second row in Table I is used to perform interleaving, where $\psi_0^{(I_1)}(n)$ is the interleaved version of the basis signal $\omega_0(n)$. The extra r bits for each symbol are

TABLE II
A SET OF INTERLEAVERS FOR DIVIDING A SYMBOL INTO EIGHT SEGMENTS

Index	Interleaver							
	1	3	5	7	8	2	4	6
0	1	3	5	7	8	2	4	6
1	1	8	4	2	5	3	6	7
2	1	2	4	7	5	8	3	6
3	1	4	7	5	2	6	3	8
4	1	2	8	3	6	4	5	7
5	1	4	8	6	2	7	3	5
6	1	5	4	6	7	3	8	2
7	1	2	7	8	4	3	5	6

converted into a decimal number q to determine the use of the q th interleaver.

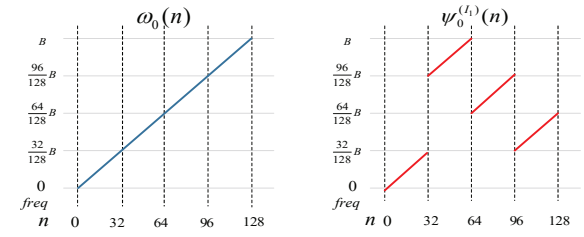


Fig. 2. The example of signals $\omega_0(n)$ and $\psi_0^{(I_1)}(n)$ with $f = 7$.

Figure 3 shows the block diagram of the EICS-LoRa transmitter. The transmitter accepts a vector X of length $r + f$ bits. Firstly, the most significant f bits go through a non-binary encoder and a LoRa modulation module to obtain a LoRa chirp symbol $\omega_l(n)$, where l is the decimal result output by the encoder. Then, the relatively less significant r bits pass a non-binary encoder to generate a decimal number q which is used to select interleaver from 2^r interleavers. Last step is to use the selected interleaver to generate interleaved LoRa chirp symbol $\psi_l^{(I_q)}(n)$ which is the transmitted signal $s_{EICS}(n)$.

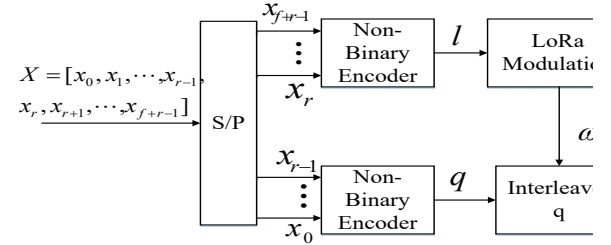


Fig. 3. Block diagram of the EICS-LoRa transmitter.

B. Demodulation of EICS-LoRa

The demodulation process of the proposed EICS-LoRa scheme is similar with ICS-LoRa's. Figure 4 presents the block diagram of demodulation process of the EICS-LoRa receiver. The received 2^r de-interleaved signals $r_{EICS}^{(I_i)}(n)$ ($i \in \{0, 1, \dots, 2^r - 1\}$) could be obtained by using the same 2^r interleavers as the transmitter. After that, these de-interleaved signals undergo the LoRa demodulation process, namely, dechirping, DFT and detection, respectively.

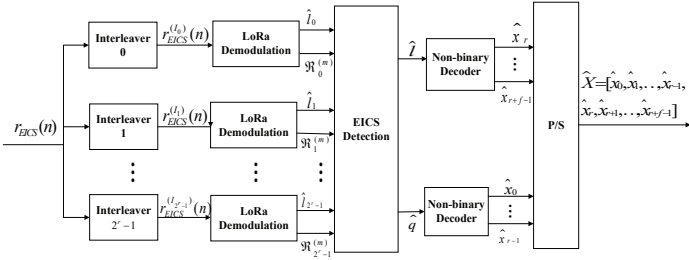


Fig. 4. Block diagram of the EICS-LoRa receiver.

According to Eq. (10) and Eq. (11), a set of \hat{l}_i , the indexes of the maximum one of each group of DFT output amplitude values could be obtained. Additionally, we could also attain the maximum values $\mathcal{R}_i^{(m)}$ of each set of DFT output amplitude values. The first step of the EICS-LoRa detection is to compare the 2^r maximum values of DFT output amplitudes and get the maximum one $\mathcal{R}^{(M)}$ within them. The index of $\mathcal{R}^{(M)}$ is \hat{q} . It means that the largest value of DFT output amplitudes of the q th interleaver is the maximum one among all $2^r \times 2^f$ DFT output amplitude values. In the second step, $\hat{l}_{\hat{q}}$ is detected with the same as the demodulation of non-binary LoRa symbol \hat{l} . The principles of the EICS-LoRa detection are as follows.

$$\mathcal{R}_i^{(m)} = \max_{0 \leq k \leq 2^f-1} (|\mathcal{R}_k^{(I_i)}|), \quad (12)$$

$$\hat{l}_i = \arg \max_{0 \leq k \leq 2^f-1} (|\mathcal{R}_k^{(I_i)}|), \quad (13)$$

$$\hat{q} = \arg \max_{0 \leq i \leq 2^r-1} (\mathcal{R}_i^{(m)}), \quad (14)$$

$$\hat{l} = \hat{l}_{\hat{q}}. \quad (15)$$

Finally, \hat{q} and \hat{l} are respectively subjected to non-binary decoder and then their results are combined to obtain the output vector \hat{X} .

IV. SIMULATION RESULTS

A. DFT outputs of EICS-LoRa

According to Eq. (4) and Eq. (5), the dechirped signal could be expressed as

$$\bar{r}_{EICS}^{(I_i)}(n|\Omega_l) = \sqrt{E_S} \cdot \bar{r}_l^{(I_i)}(n) + \sum_{m=0}^{2^f-1} \eta_m \cdot \bar{r}_m^{(I_i)}(n), \quad (16)$$

where $\bar{r}_{EICS}^{(I_i)}(n|\Omega_l)$ is the dechirped received signal which is interleaved by the i th interleaver and l is the transmitted non-binary LoRa symbol. Based on Eq. (6), the k th DFT output $\mathcal{R}_k^{(I_i)}$ of $\bar{r}_{EICS}^{(I_i)}(n|\Omega_l)$ is derived as

$$\mathcal{R}_k^{(I_i)} = \mathcal{F}_k(\bar{r}_l^{(I_i)}) \cdot \sqrt{E_S} + \sum_{m=0}^{2^f-1} \eta_m \cdot \mathcal{F}_k(\bar{r}_m^{(I_i)}), \quad (17)$$

where $\mathcal{F}_k(\bar{r}_m^{(I_i)})$ is the k th ($k \in \{0, 1, \dots, 2^f-1\}$) DFT output of the dechirped signal $\bar{r}_m^{(I_i)}(n)$. According to Eq. (7), the magnitude reaches the maximum value when $k = l$.

Figure 5 shows an example of a series of DFT output amplitude values when four interleavers are used without considering channel noise. From top to bottom are DFT

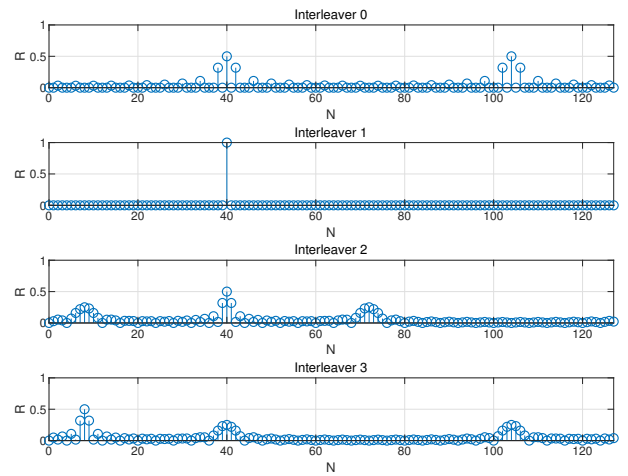


Fig. 5. An example of DFT output amplitude values of EICS-LoRa with $f=7$.

output amplitude values of the interleaved signals generated by interleavers numbered from 0 to 3. It is easy to observe that the largest DFT output amplitude value in the second set of data is the maximum one which is corresponding to the number of interleaver adopted at transmitter.

B. BER performance of EICS-LoRa

We use the AWGN channel to test the bit error rate (BER) performance of the proposed EICS-LoRa scheme. We compare the BER performance when the number of additional bits carried by a LoRa symbol $r \in \{2, 3, 5\}$ and $f = 7$. The simulation results are shown in Fig. 6. From the figure, we can see that the BER decreases persistently as the SNR increases. In order to obtain the same BER performance, the sensitivity difference for the different r becomes more and more obvious as the increase of the SNR. These show that the BER performance would be fleetly worsen when r is large (eg. $r \geq 5$). The reason is that as the increase of the number of candidate interleavers, the orthogonality among the interleaved chirp signals may not be guaranteed, which results in a larger BER.

In addition, BER curves of LoRa and ICS-LoRa are plotted in Fig. 6. It is shown that EICS-LoRa ($r = 2$) sacrifices about 0.44dB and 0.81dB of sensitivity relative to ICS-LoRa and LoRa at BER level 10^{-4} . The results illustrate that the proposed EICS-LoRa scheme increases at least 2 bits per symbol at the cost of adding about 0.8dB to the channel environment requirements.

Figure 7 shows the BER performance when $f = 10$ and $r \in \{2, 3, 4\}$. The results are roughly the same as those when $f = 7$. The SNR gaps among the three schemes are narrowed at the same BER level. To achieve a BER at 10^{-4} , EICS-LoRa sacrifices about 0.51dB of sensitivity compared to LoRa. The SNR gap is reduced to about 0.26dB compared to ICS-LoRa.

The tradeoff between the data rate gain and the SNR loss across SFs ranging from 7 to 12 is summarized in Table III.

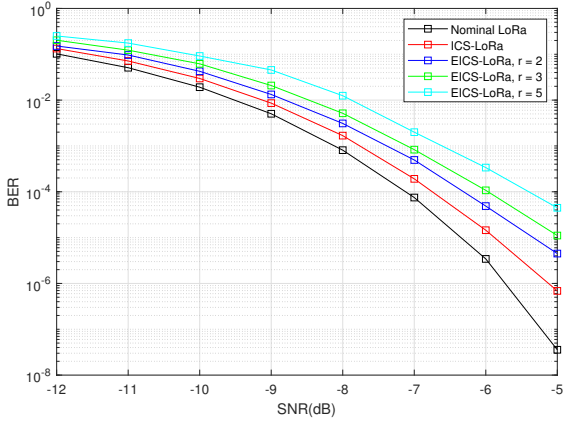


Fig. 6. BER performance of EICS-LoRa with $f = 7$.

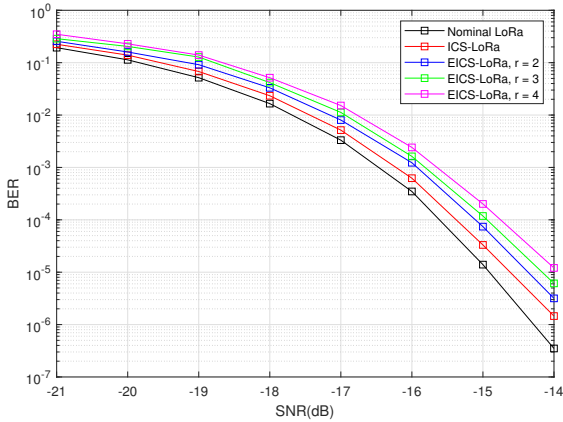


Fig. 7. BER performance of EICS-LoRa with $f = 10$.

According to [12], the data rate of LoRa is given as

$$C = f \times \frac{B}{2^f}, \quad (18)$$

where C denotes the data rate of LoRa. It means that f bits per LoRa symbol are transmitted at a symbol rate of $B/2^f$. Based on that, the rate gain of EICS-LoRa is calculated by $(r/f) \times 100\%$, where r is the number of additional bits every EICS-LoRa symbol carries. The performance gap between the EICS-LoRa scheme and LoRa is evaluated assuming a receiver sensitivity at BER $P_b = 10^{-4}$. By comparing the data in the table, it can be seen that the SNR loss of EICS-LoRa is almost less than 1.7dB when r takes a value from 2 to 5. With the increase of f , the SNR loss is decreasing.

C. Resistance to co-SF interference

It is well known that the LoRa signals with different SFs are quasi-orthogonal and the interference between them could actually be ignored (unless the transmitted signal and the interference signal have the same chirp rate [14]), so that the LoRa system supports multiple simultaneous logical networks [15]. However, unlike the interference with different SFs, LoRa signals with the same SF (co-SF) have greater impact on the desired signal due to their cross-correlation. A good way

TABLE III
RATE GAIN AND BER PERFORMANCE GAP OF EICS-LORA (BER AT 10^{-4})

SF	$r = 2$		$r = 3$	
	Rate gain	Performance gap	Rate gain	Performance gap
7	28.57%	-0.81dB	42.86%	-1.15dB
8	25.00%	-0.69dB	37.50%	-0.83dB
9	22.22%	-0.56dB	33.33%	-0.79dB
10	20.00%	-0.51dB	30.00%	-0.67dB
11	18.18%	-0.41dB	27.27%	-0.56dB
12	16.67%	-0.30dB	25.00%	-0.46dB
		$r = 4$	$r = 5$	
SF	Rate gain	Performance gap	Rate gain	Performance gap
7	57.14%	-1.37dB	71.43%	-1.72dB
8	50.00%	-1.08dB	62.50%	-1.49dB
9	44.44%	-1.05dB	55.56%	-1.45dB
10	40.00%	-0.87dB	50.00%	-1.34dB
11	36.36%	-0.72dB	45.45%	-1.06dB
12	33.33%	-0.64dB	41.67%	-0.86dB

to solve the burst error of signals is the interleaving method [16]. Therefore, the key signal processing method used in EICS-LoRa, namely chirp signals interleaving method, should have good performance in resisting co-SF interference. In this subsection, simulation results will be used to illustrate this point.

It is shown in [15] that the reason why the LoRa gateway can maintain the same coverage of the LoRa signal under co-SF interference is mainly that the signal-to-interference ratio (SIR) of the signal of interest exceeds a given threshold. Referring to [8] and [17], the threshold of SIR is set to 6dB in our simulations.

We consider an EICS-LoRa transmitted signal $s_{EICS}(nT)$ which is interfered by other EICS-LoRa signals with co-SF. Similar to [15], we assume that the transmitters of EICS-LoRa are not synchronized, resulting in a random displacement of τ samples between the desired signal and the interference signal. The EICS-LoRa interference signal is expressed as

$$I(i_1, i_2, \tau, nT) = \begin{cases} \omega_{i_1}(nT)/\sqrt{\gamma} & 0 \leq n < \tau \\ \omega_{i_2}(nT)/\sqrt{\gamma} & \tau \leq n < 2^f, \end{cases} \quad (19)$$

where γ represents the SIR of the interference signal $I(i_1, i_2, \tau, nT)$ relative to the transmission signal $s_{EICS}(nT)$, which is 6dB here. The interference signal means the transmission signal is interfered by the EICS-LoRa signal $\omega_{i_1}(nT)$ at the first τ sampling points and is interfered by the EICS-LoRa signal $\omega_{i_2}(nT)$ at the next $2^f - \tau$ sampling points ($i_1, i_2 \in \{0, 1, \dots, 2^f - 1\}$). For simplicity but without loss of generality, we assume that $0 \leq \tau \leq 2^{f-1}$, which means that the number of samples of the second interference signal is greater than the number of samples of the first interference signal.

Figure 8 shows the simulation results when $f = 8$ and the number of additional bits per symbol r is set to 2 or 3. As shown in the figure, solid lines and dashed lines respectively represent the BER performance of the two schemes without and with co-SF interference. We could observe that the SNR loss caused by co-SF interference of LoRa is slightly larger than that of EICS-LoRa. For example, at BER level of 10^{-4} ,

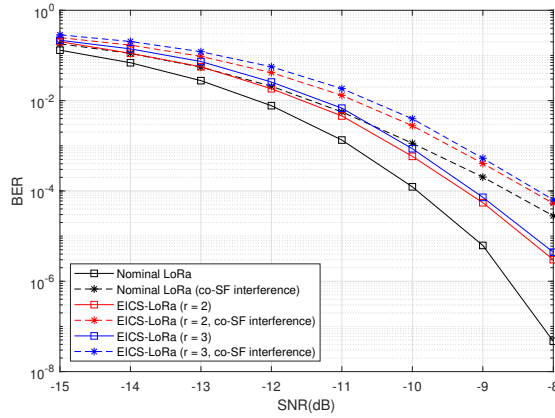


Fig. 8. BER performance with and without co-SF interference, with $f = 8$.

LoRa sacrifices about 1.28dB of sensitivity, while EICS-LoRa sacrifices about 0.94dB and 0.92dB sensitivity when $r = 2$ and $r = 3$, respectively. It could be inferred that the interleaving method introduced in the EICS-LoRa scheme has a better inhibitory effect on the impact of co-SF interference compared with LoRa. In other words, the interleaving module in EICS-LoRa makes it have a good ability to resist co-SF interference.

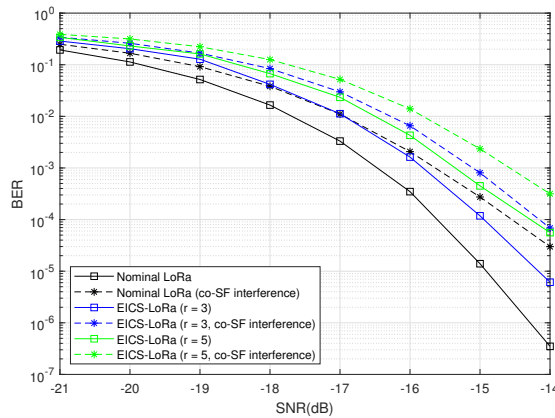


Fig. 9. BER performance with and without co-SF interference, with $f = 10$.

The simulation results shown in Fig. 9 for $f = 10$ and $r = 3, 5$ could also support this conclusion. LoRa sacrifices approximately 1.07dB sensitivity at BER level of 10^{-4} . In contrast, for the same constraints, EICS-LoRa sacrifices about 0.78dB and 0.80dB sensitivity when $r = 3$ and $r = 5$, respectively. Compared Fig. 8 and Fig. 9, it is shown that the proposed EICS-LoRa scheme sacrifices less sensitivity with the increase of f .

V. CONCLUSION

Based on the ICS-LoRa scheme, this paper introduces multiple interleavers to increase the number of bits carried by each LoRa symbol. Compared with LoRa, the maximum rate gain of the proposed scheme could reach up to 71.43% at content of complexity increase and SNR loss. When the number of additional bits per symbol is set from 2 to 5, the

SNR loss is about 0.3 to 1.7dB for $f \in [7, 12]$. It is worth noting that an increase in the number of transmitted bits may bring more SNR loss while an increase in f could reduce SNR loss. Therefore, there should be a good trade-off between f and r . Moreover, EICS-LoRa is less sensitive to co-SF interference than LoRa due to the interleaving method.

ACKNOWLEDGMENT

This work was supported in part by the Natural Science Foundation (NSF) of China under Grant No. 61871337.

REFERENCES

- [1] C. Goursaud and J.-M. Gorce, "Dedicated networks for IoT : PHY/MAC state of the art and challenges," *EAI Endorsed Trans. Internet Things*, vol. 1, no. 1, pp. 1-11, 2015.
- [2] M. Centenaro, L. V angelista, A. Zanella, and M. Zorzi, "Long-range communications in unlicensed bands: The rising stars in the IoT and smart city scenarios," *IEEE Wireless Commun.*, vol. 23, no. 5, pp. 60-67, Oct 2016.
- [3] J. P . Bardyn, T. Melly, O. Seller, and N. Sornin, "IoT: The era of LPWAN is starting now," in *Proc. 42nd Eur . Solid-State Circuits Conf.*, 2016, pp. 25-30.
- [4] B. Reynders et al., "Range and coexistence analysis of long range unlicensed communication," in *Proc. 23rd International Conference on Telecommunications (ICT)*, 2016, pp. 1-6.
- [5] L. V angelista, "Frequency shift chirp modulation: The LoRa modulation," *IEEE Signal Process. Lett.*, vol. 24, no. 12, pp. 1818-1821, Dec. 2017.
- [6] B. Reynders and S. Pollin, "Chirp spread spectrum as a modulation technique for long range communication," in *Proc. Symp. Commun. V eh. Technol.*, 2016, pp. 1-5.
- [7] M. Hanif and H. H. Nguyen, "Frequency-Shift Chirp Spread Spectrum Communications with Index Modulation," *IEEE Internet Things J.*, May. 2021, pp. 1-1.
- [8] O . Georgiou and U . Raza, "Low power wide area network analysis: Can lora scale?" *IEEE Wireless Commun. Lett.*, vol. 6, no. 2 , pp. 162-165, April 2017.
- [9] R. Bomfin, M. Chafii, and G. Fettweis, "A novel modulation for IoT: PSK-LoRa," in *Proc. IEEE V eh. Technol. Conf.*, Apr. 2019, pp. 1-5.
- [10] T. T. Nguyen, H. H. Nguyen, R. Barton, and P . Grossetete, "Efficient design of chirp spread spectrum modulation for low-power wide-area networks," *IEEE Internet Things J.*, vol. 6, pp. 9503-9515, Dec. 2019.
- [11] M. Hanif and H. H. Nguyen, "Slope-shift keying LoRa-based modulation," *IEEE Internet Things J.*, vol. 8, no. 1, pp. 211-221, Jan. 2021.
- [12] T. Elshabrawy and J. Robert, "Interleaved chirp spreading LoRa-based modulation," *IEEE Internet Things J.*, vol. 6, no. 2, pp. 3855-3863, Apr. 2019.
- [13] T. Elshabrawy and J. Robert, "Closed-form approximation of LoRa modulation BER performance," *IEEE Commun. Lett.*, vol. 22, no. 9, pp. 1778-1781, Sep. 2018.
- [14] B. Dunlop, H. H. Nguyen, R. Barton and J. Henry, "Interference Analysis for LoRa Chirp Spread Spectrum Signals," in *Proc. 2019 IEEE Canadian Conference of Electrical and Computer Engineering (CCECE)*, 2019, pp. 1-5.
- [15] T. Elshabrawy and J. Robert, "Analysis of BER and coverage performance of LoRa modulation under same spreading factor interference," in *Proc. 2018 IEEE 29th Annual International Symposium on Personal, Indoor and Mobile Radio Communications (PIMRC)*, 2018, pp. 1-6.
- [16] H. Murata and S. Yoshida, "Co-channel interference canceller for interleaved coded modulation in the presence of intersymbol interference," in *Proc. 48th IEEE Vehicular Technology Conference*, 1998, pp. 1636-1640 vol.2.
- [17] J. T. Lim and Y . Han, "Spreading factor allocation for massive connectivity in lora systems," *IEEE Commun. Lett.*, vol. 22, no. 4, pp. 800-803, April 2018.